*Materials Research*. 2023; 26(suppl. 1): e20230084
DOI: https://doi.org/10.1590/1980-5373-MR-2023-0084



# Microstructural Characterization of a Component Manufactured by Hybrid Casting of Two Different Ferrous Alloys

**E.L.S. Junior[a]*, R. Leibholz[a], M.S.F. Lima[a], K. Zilnyk[a]**

[a]*Instituto Tecnológico de Aeronáutica (ITA), Departamento de Materiais e Processos (IEM-MP), 12228-900, São José dos Campos, SP, Brasil.*

Received: January 16, 2023; Revised: March 24, 2023; Accepted: May 03, 2023

Hybrid casting is a new fabrication concept that can reduce costs and production time of large tools, such as stamping tools for the automotive industry. In this work, we analyzed a hybrid material composed of a high chromium cast iron (HCCI) and a low carbon steel (WCB). SEM analyses indicate that the interface is free of non-metallic inclusions and porosities. The metallurgical bonding between alloys is confirmed by the diffusion of chromium and carbon from HCCI to WCB. Vickers microhardness, EDS and XRD confirmed the presence of M7C3 carbides in the HCCI and at the interface. One set of the samples was submitted to regular quenching in calm air and tempering, while another set was additionally submitted to subzero quenching before tempering. In both cases, a slight reduction of the HCCI hardness and an increase of the interface hardness were observed. The subzero treatment was effective to reduce the amount of retained austenite at the HCCI and limiting its hardness reduction. WCB microstructure and hardness showed no significative change, making it an ideal material to use with HCCI in hybrid casts. The results showed that is possible to produce bimetallic reliable components for industrial applications by means of hybrid casting.

**Keywords:** *Hybrid Casting, Hardness, High Chromium Cast Iron (HCCI).*

## 1. Introduction

The engineering industry is always looking for new ways to reduce costs while producing components with special properties. One new interesting casting process is the Hybrid Casting (HC), also known as Bi-Metallic Casting. The HC is the technique of pouring two materials with different chemical compositions and microstructures into the same mold (liquid-liquid system), usually using the full molding process, ensuring a continuous interface in a defined position without mixing and maintaining the integrity of the mold[1]. These nomenclatures may also be used for liquid-solid system where a granular material or an insert is inserted in a mold with just one pouring channel for a single liquid metal[2]. Figure 1 shows the schematic representation of the process.

Despite not being extensively used in the tooling industry yet, the HC process can drastically reduce costs with machining and assembling. This is very important for industries that require large tooling, such as the automotive industry. The total production time of heavy manufacturing tools, such as stamping tools to produce Class A surfaces or structural components, can also be reduced. Furthermore, it can increase efficiency and tool life while reducing raw material costs. This is possible by using a more resistant and higher value material in the area subject to wear, while in other parts of the component a cheaper and less resistant material can be used[3], since in components where a high corrosion and abrasive wear resistance are required expensive alloying elements such as Ni, Co, Ti and Cr are commonly used[1,2]. The HC technology is an economical way to make high efficient tools without the use of welding or thermal spraying.

Seeking to better understand the hybrid casting process, in this study a bi-metalic component made of low carbon steel (WCB steel) and high chromium cast iron (HCCI) was produced and analyzed. Among the HCCI material family, there are hypoeutectic alloys containing 10-30% of Cr and 2-3.5% of C. HCCI with Cr between 18-22% are the most used, as they combine high mechanical strength and wear resistance, in addition to high corrosion resistance and high hardness. This makes it ideal for use in several applications in the tooling industry, such as mill hammers, mining equipment and stamping tools. These properties are achieved with a microstructure composed of primary carbides distributed in a martensitic matrix with some retained austenite[4-6]. These carbides present in the microstructure can be presented in the form of M7C3 compounds, such as (Cr, Fe)7C3 which can have a hardness of up to 1800 HV, or in the form of M23C6 with a hardness of up to 1650 HV. In both cases, they provide a high wear resistance to the material[4-8].

This work presents a characterization of a hybrid component microstructure, analyzed as-cast, after quenching in calm air and tempering, with and without additional subzero quenching. Since both alloys will invariably have to undergo the same heat treatments, generally specified according to the highest strength alloy, it's important to ensure that the support material can withstand such heat treatment without harmful consequences to their microstructure. Scanning electron microscopy (SEM) coupled with energy dispersive spectroscopy (EDS) was

*e-mail: elsjrsilva@gmail.com

performed to characterize the 3 regions of the component (WCB-Interface-HCCI), with a special focus on the interface. Hardness tests and X-ray diffraction (XRD) were also performed, and the results compared to Scheil-Gulliver calculations of the casting microstructure performed using the CALPHAD (Calculation of Phase Diagram) approach.

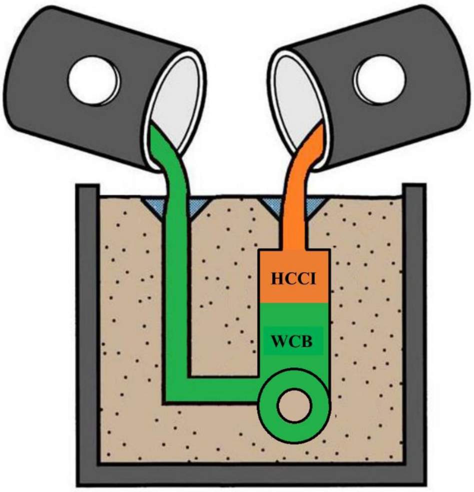


**Figure 1.** Schematic representation of the hybrid casting process.

## 2. Experimental Procedure

The full molding sand casting process, with a consumable expanded polystyrene model (lost foam), was used to manufacture the hybrid component schematically shown in Figure 2. The compositions of the two alloys and their pouring temperatures are shown in Table 1. The mold size was 1 $m^3$ (1x1x1 $m^3$), about to 180 Kg of WCB was added to an induction melting furnace and 50 Kg of HCCI was melted into a second induction melting furnace. The first material to be added to the mold was WCB at a temperature close to 1550 °C, after the WCB the HCCI was added through a second feed channel in a temperature of 1450 °C, as shown in Figure 1. Both materials were added in liquid state with a difference about of 100 °C, used to guarantee the formation of the interface without mixing the two materials and granting the quality of the component.

Thermodynamic calculations were performed using the CALPHAD approach in the Thermo-Calc® software coupled with the TCFE9® database. Specifically, The Scheil-Gulliver model was employed to calculate the out-of-equilibrium solidification path of both materials and the interface[9-11]. The chemical compositions given in Table 1 were used for the two materials and their arithmetic average was considered as the composition of the interface.

Samples were cut from the hybrid component, from regions containing the individual alloys and from the interface, using an electrical discharge machine. All samples were heated to

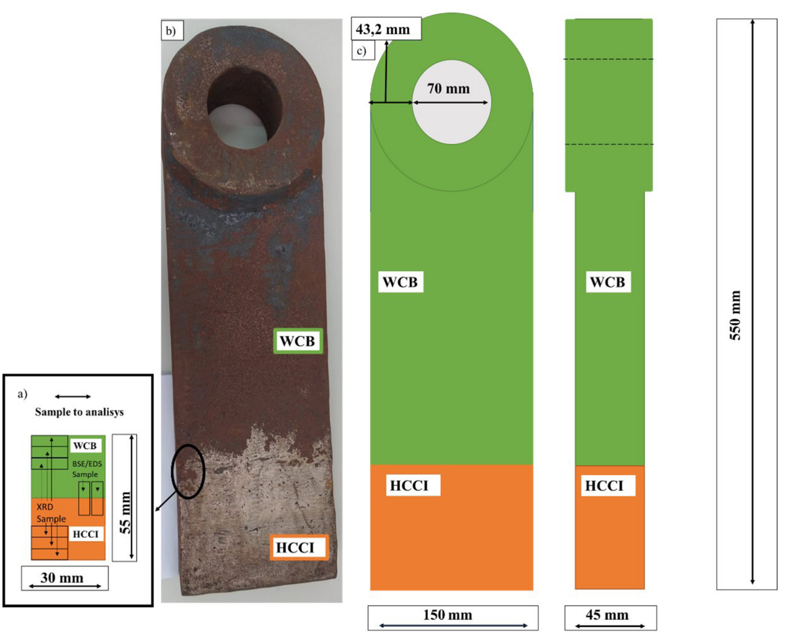


**Figure 2.** a) Area of study: XRD and BSE/EDS samples, b) Hybrid component after cast and c) schematic representation with the component dimensions.

**Table 1.** Materials composition and process parameters.

| Wt% | C | Si | Mn | Cr | Fe | Pouring temperature |
|---|---|---|---|---|---|---|
| WCB | 0,25 | 0,60 | 0,70 | - | Bal. | ≅1550 °C |
| HCCI | 3,00 | 1,00 | 1,00 | 22,00 | Bal. | ≅1450 °C |

980°C at a rate of 10°C/min and kept at this temperature for 30 minutes. Both samples were quenched in calm air. One of the samples was submitted to a subzero treatment in liquid nitrogen, close to 190°C for 30 minutes. Afterwards, both group of samples were tempered at 260 °C for 120 minutes.

Subsequently, the samples were submitted to the conventional metallographic preparation process, being grinded with 400, 600, 800, 1200 and 2500 grit SiC paper and polished with 3 and 1µm diamond paste and 0.04 µm colloidal silica suspension and etched with nital 2% for a few seconds.

The samples were analyzed by SEM in a Tescan Vega 3 XMU, using backscattered electrons (BSE) imaging mode and energy dispersive X-ray spectroscopy (EDS), to study the interface formed between the two materials and their microstructure in the as-cast material and after the heat treatments. The EDS maps aimed to show the distribution of carbides present in the HCCI, while the line EDS was used to identify a possible diffusion of carbon, chromium, and other alloying elements between the alloys.

To observe possible changes in the phase fractions during heat treatment, the samples were analyzed by XRD in a Panalytical Empyrean diffractometer using Cu-Kα radiation followed by Rietveld refinement. The XRD was performed at each material individually, in 15 x 5 $mm^2$ samples collected from regions close to the interface but not encompassing it, as shown in Figure 2. Hardness maps were made by Vickers microindentation in an automatized Emcotest DuraScan G50 with a load of 0.025 HV and a dwell time of 15 s. Two spacings were used for the hardness maps: 0.5 mm for maps throughout the sample and 0.05 mm in the interface region.

## 3. Results and Discussions

The solidification path of HCCI and WCB was simulated using the Thermo-Calc® software coupled with the TCFE9® database, as shown in Figure 3. In HCCI, solidification begins with the formation of M7C3 carbides followed by austenite (Figure 3a). The literature reports that, during the solidification of HCCIs different carbides may be formed depending on the chemical composition of the alloy. Hashimoto et al.[10] studied a Fe-5%Cr-5%V-5%Mo-5%W-5%Co (%Wt) HCCI and found that V, W, or Mo was responsible for the formation of carbides. Usually, the first carbides that start to solidify were nodular MC or plate-like M2C, solidifying as eutectic carbides, and in sequence there was the formation of austenite. The primary carbides can react with austenite and transform into both M6C and M7C3. This transformation can also occur during heat treatments. Matsubara et al.[11] studied different HCCI containing 20%Wt of carbide- forming elements. Alloys with lower Cr and higher V, Mo and W also showed MC and M2C, while in the higher Cr (17%Wt) alloy the pro-eutetic M7C3 carbide was formed, followed by a L → M7C3 + austenite eutetic reaction[12]. Doğan et al.[13] investigated hypoeutetic, eutetic and hypereutetic HCCIs, containing 15% or 26%Wt Cr. Despite the carbon content, all alloys containing 26%Wt of Cr formed only M7C3, while the alloys with 15%Cr showed both M7C3 and peritetic M3C. In both hypoeutetic alloys, pro-eutetic austenite was observed.

Figure 3b) shows the ferritic-austenitic solidification path of the WCB steel. Considering the dilution of equal parts of the two alloys at the interface (caused mainly by solute diffusion since the pouring temperature were chosen to avoid major mixing of the liquid metals), the solidification path of this region is shown in Figure 3c. The lower content of alloying elements promotes the formation of a large amount of austenite before starting the formation of M7C3 carbide particles. Despite the reduced Cr content, no other carbide phase is formed.

Figure 4 shows the alloys interface on the as-cast material observed by OM and SEM at different magnifications, after nital chemical etching. A well-consolidated, but not straight, interface can be seen. One of the challenges of the hybrid casting process, is to guarantee the bound of the two materials, the interface waviness helps in the mechanical interlocking of the alloys, increasing its reliability, since it increases the contact surface between the two alloys[2]. Very small particles, about 500 nm, are visible at the interface but not in the base materials.

Figure 5 shows the EDS maps collected at the interface. In HCCI, the presence of points rich in chromium and carbon is noted. Because the high amount of chromium and few other alloying elements, the M7C3 carbides are the ones that preferentially are formed in this alloy, which was also predicted by the thermodynamic calculation[1-9]. In the WCB, a pearlitic microstructure can be seen. Figure 6 shows an EDS line scan, where the variation in carbon and chromium composition at the interface can be seen. The diffusion from

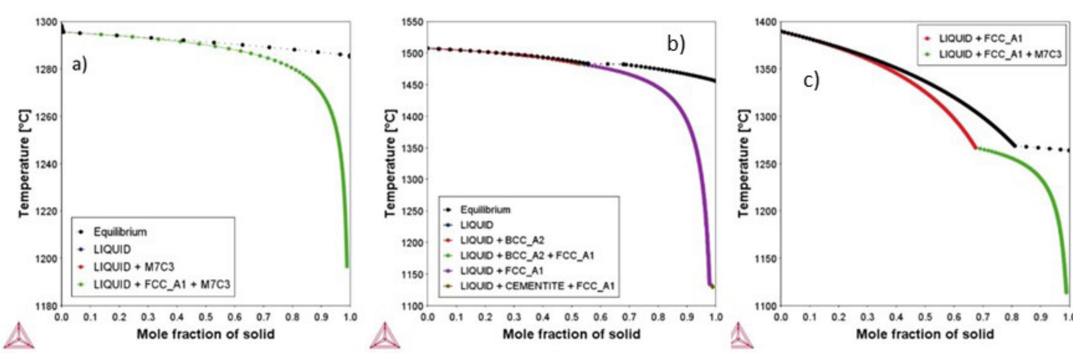


**Figure 3.** Solidification simulation of a) HCCI, b) WCB steel and c) HCCI + WCB interface.

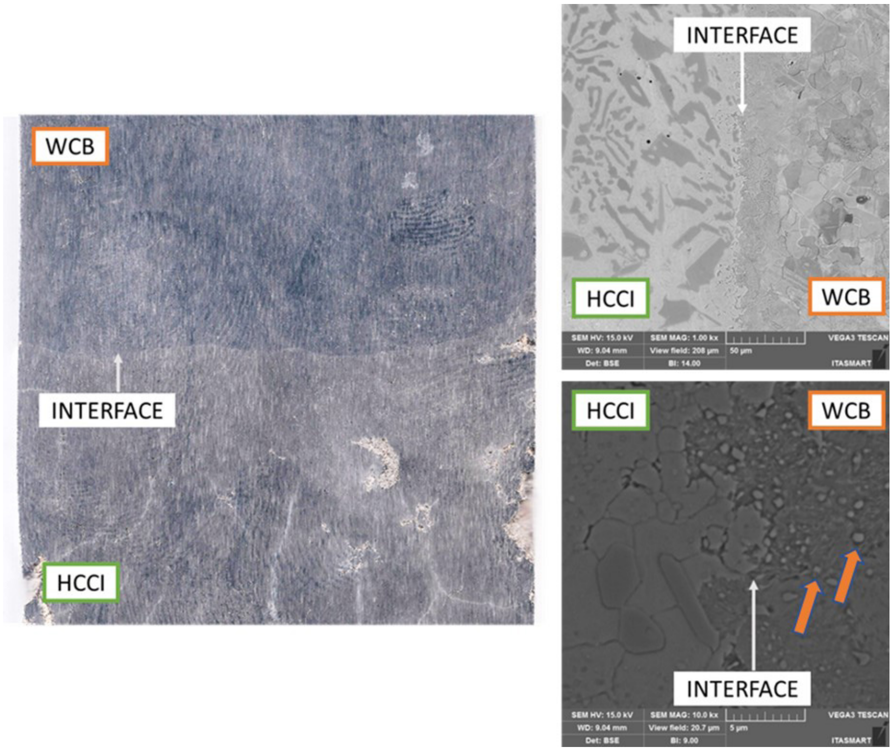


**Figure 4.** SEM images of the interface. Arrows point to fine particles present only at the interface.

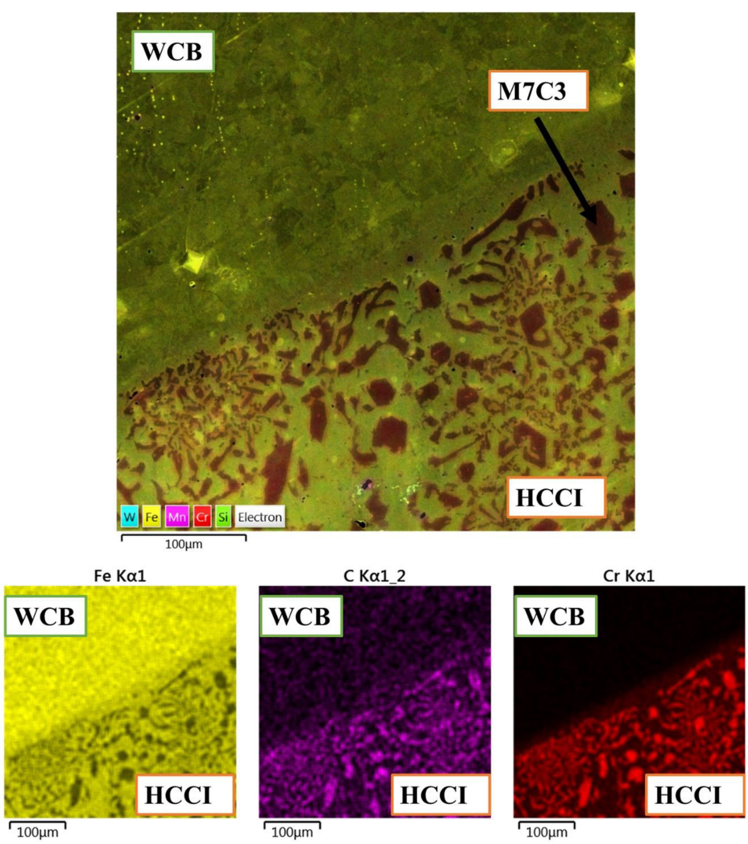


**Figure 5.** SEM-EDS maps of the interface.

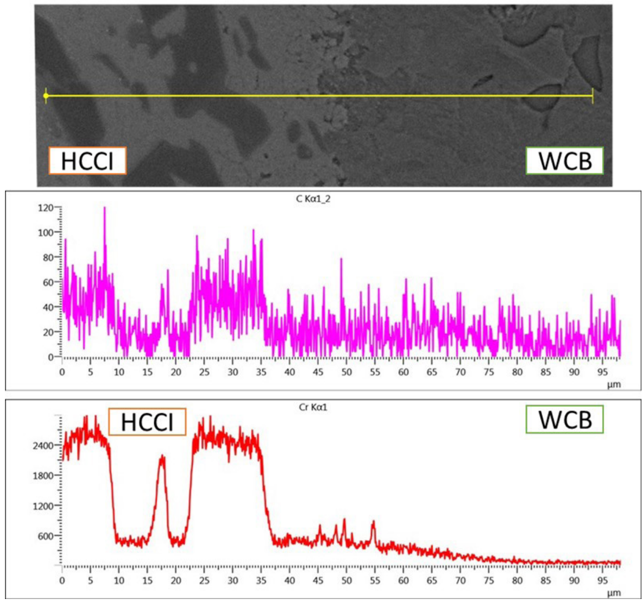


**Figure 6.** EDS line of the interface.

the C and Cr-rich HCCI towards the WCB steel can be seen for both elements, but more clearly for Cr because of its higher content and atomic number ($Z_{Cr} = 24$, $Z_C = 6$). The fine M7C3 carbides seen in Figure 4 are observable in the WCB side of the interface in Figure 4c. These particles correspond to the Cr-rich areas in the line scan (between 45 and 55 µm) and proves the occurrence of Cr diffusion into the WCB.

Hardness analyses were also carried out to determine how this property behaves at the interface and to determine what would be the positions of the carbides. Figure 7 shows the hardness maps made across the entire sample and in the interface region. Hardness values for the carbides vary between 1200-1800 HV, which indicates that they can be both transverse and longitudinal M7C3 carbides[12]. At the interface, there is a gradual increase in hardness, where in the WCB there is an average hardness of 200 HV, as we advance in the interface the hardness increases to 500-700HV until reaching the HCCI, where the martensitic matrix with chromium carbides is responsible for the very high hardness[1,9-11].

After characterizing the as-cast material, two set of samples were submitted to austenitization. One was quenched at calm air and another one by subzero quenching. In both cases, the same tempering parameters were used afterwards.

In the Figure 8 is showed the BSE and EDS image of the quenched and tempered sample. Figure 9 shows the BSE and EDS image of sub-zero and tempered sample. In both cases there is an increase in the width of the interdiffusion zone between the two alloys. The increase in the interdiffusion zone, because of the diffusion of C and Cr from the HCCI to the WCB steel, gives the impression of carbide refinement at the interface, but no significant dilution of the coarse M7C3 carbide particles was observed. The carbides located at the interdiffusion zone are smaller, compatible with the ones found at the interface of the as-cast samples.

Figure 10 to Figure 13 shows the hardness map of all samples heat treated. Comparing Figure 10 with Figure 7,

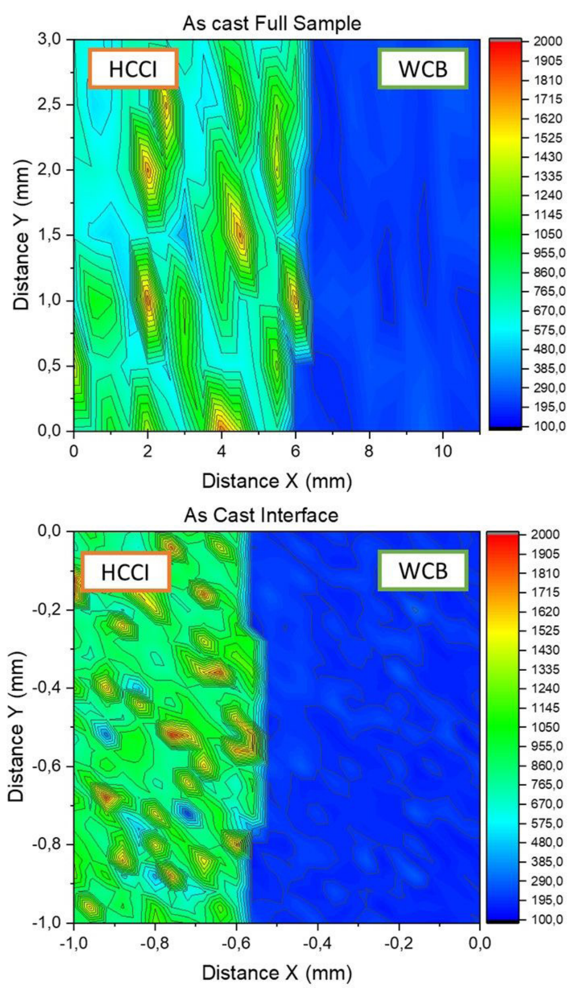


**Figure 7.** Vickers hardness test 0,025HV of the as cast full sample and interface.

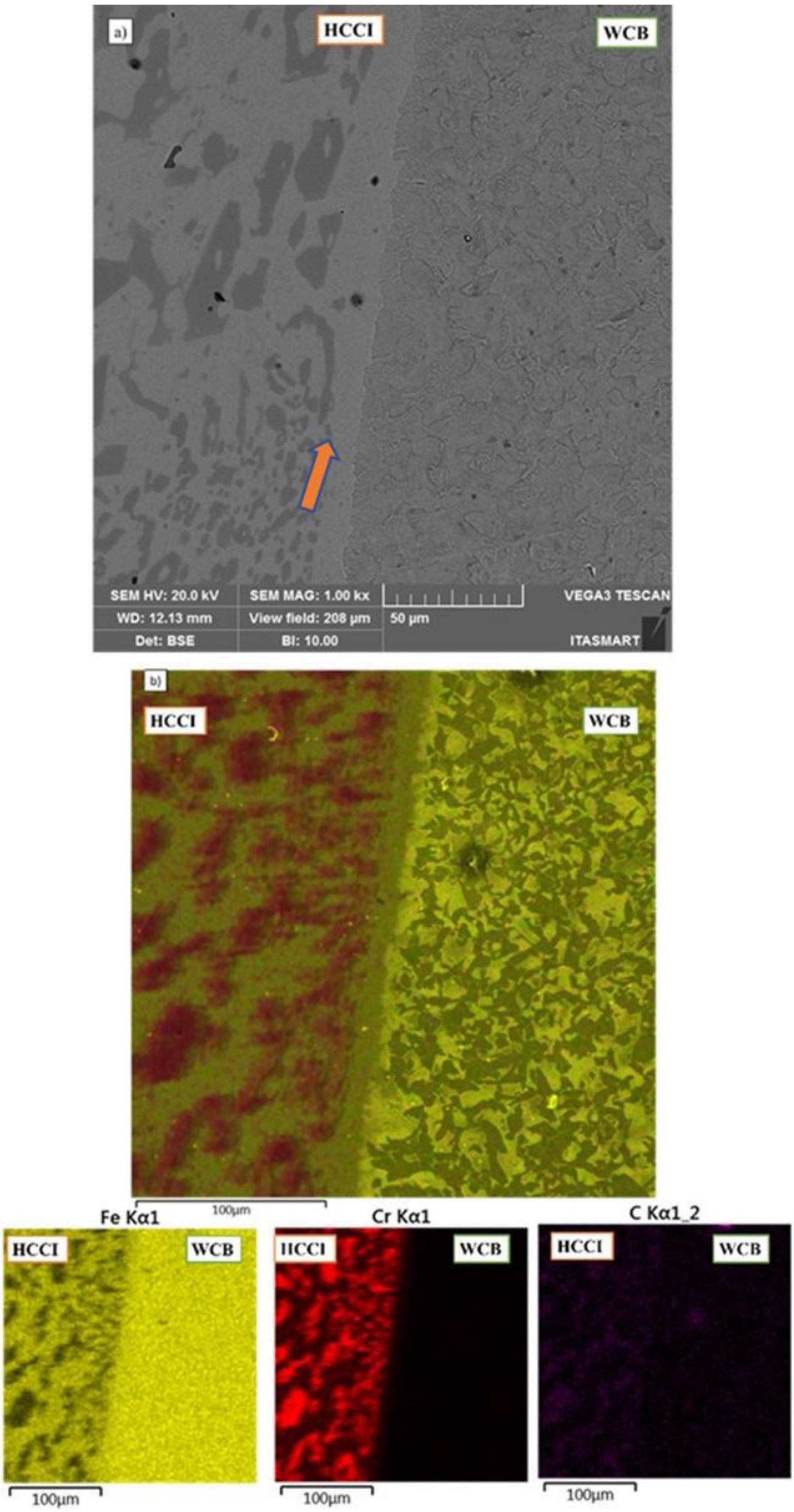


**Figure 8.** a) BSE image of the sample after calm-air quenching and tempering and, b) EDS image with Fe, Cr and C distribution. The arrow points to the interdiffusion zone.

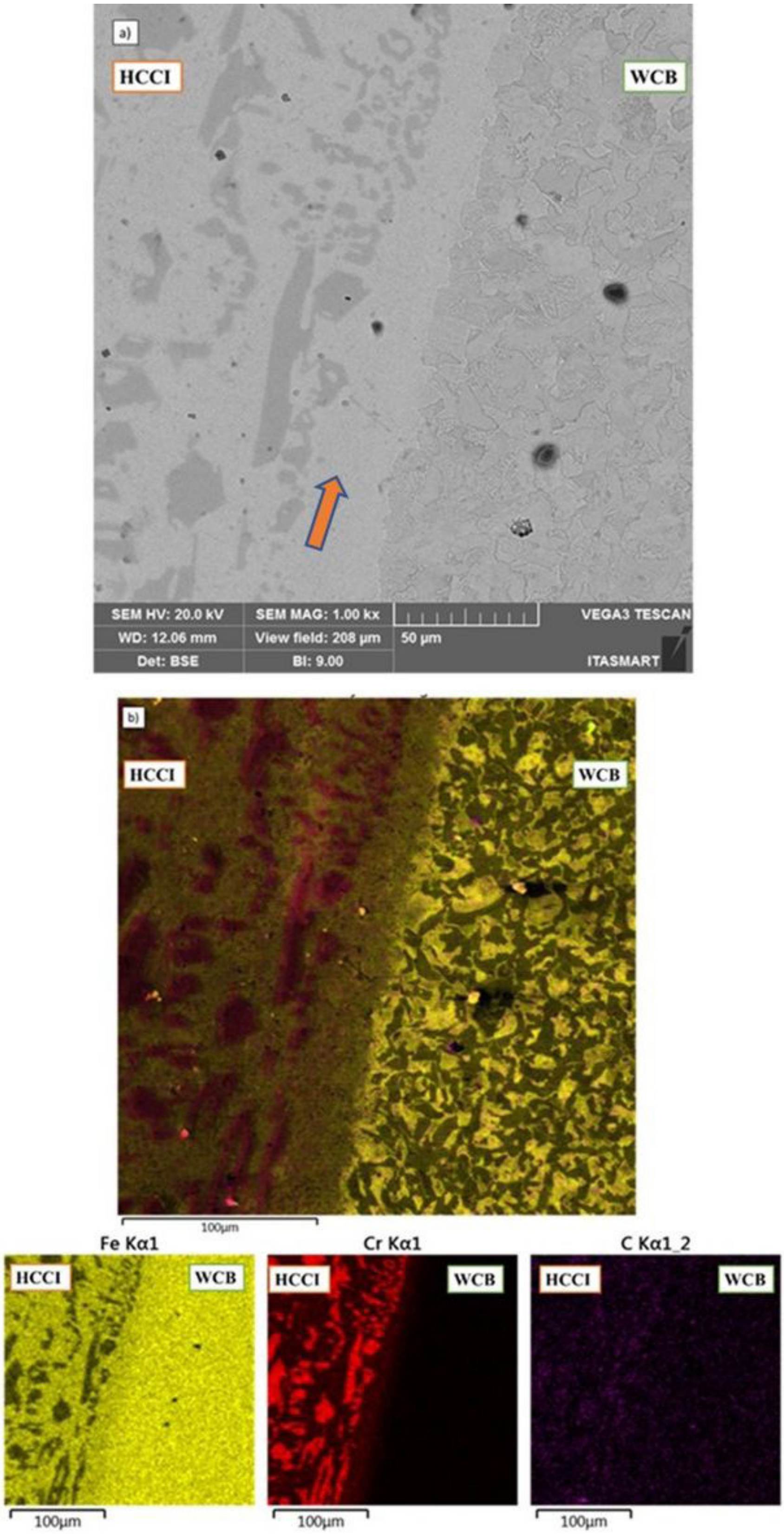


**Figure 9.** a) BSE image of the sample after calm-air quenching, sub-zero quenching and tempering, and b) b) EDS image with Fe, Cr and C distribution. The arrow points to the interdiffusion zone.

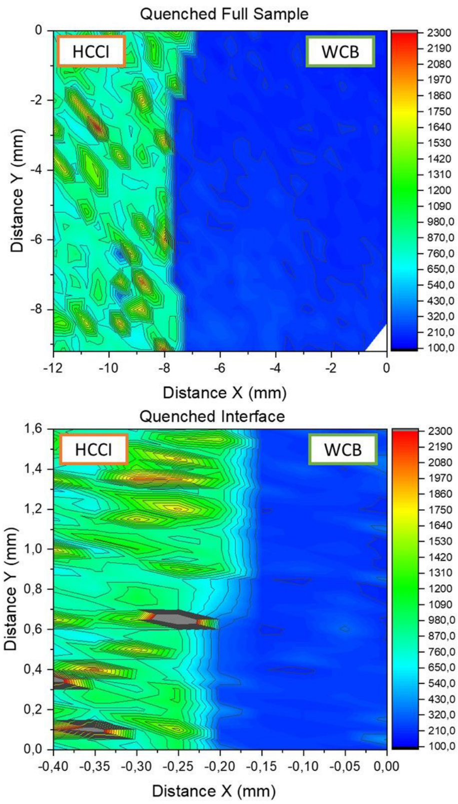


**Figure 10.** Vicker's Hardness map of the quenched sample.

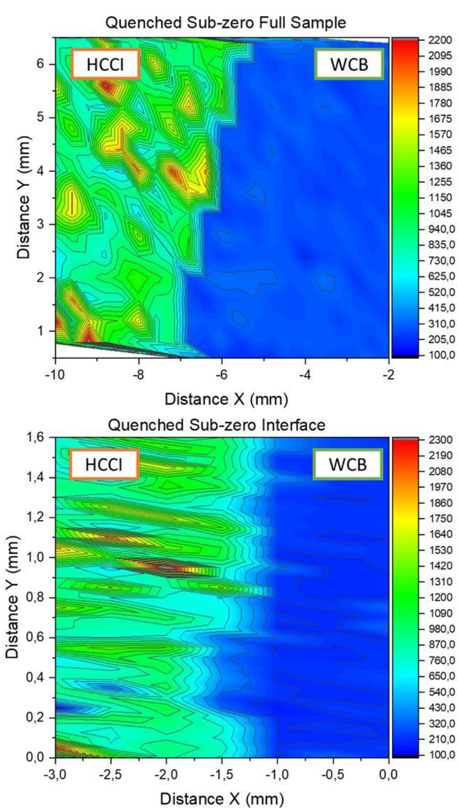


**Figure 11.** Vickers hardness map of quenched and sub-zero treatment samples.

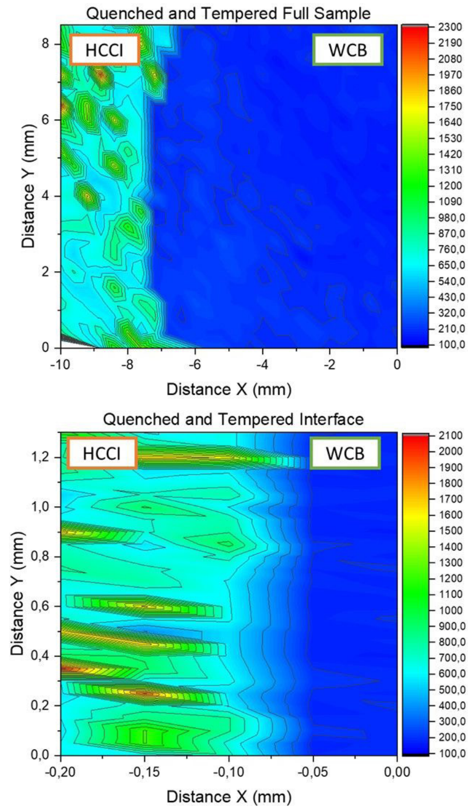


**Figure 12.** Vickers hardness map of quenched and tempered samples.

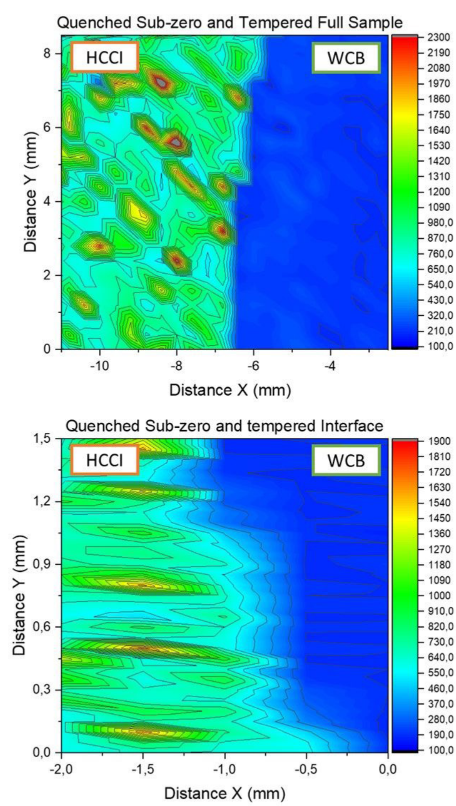


**Figure 13.** Vickers hardness map of quenched, sub-zero treatment, and tempered samples.

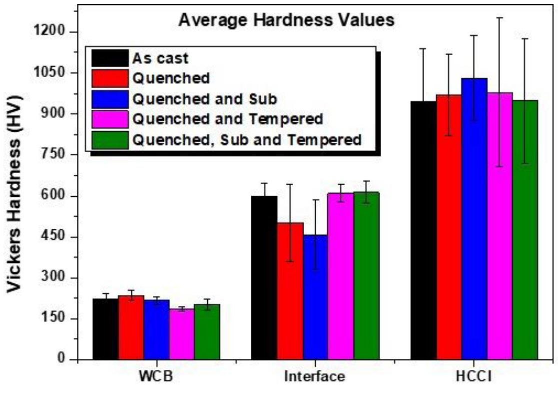


**Figure 14.** Average Hardness Values of the component.

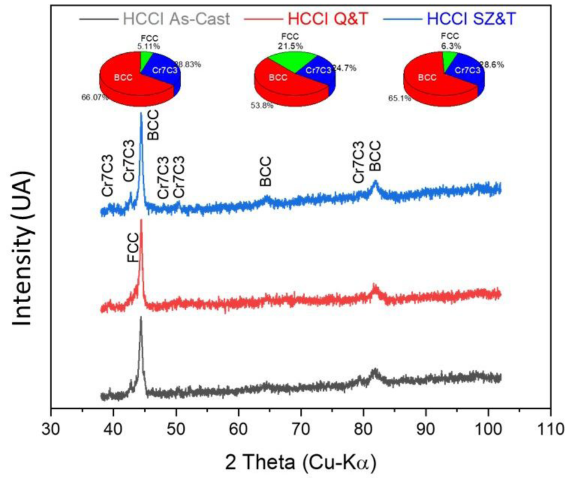


**Figure 15.** XRD of HCCI as cast and after heat treatment.

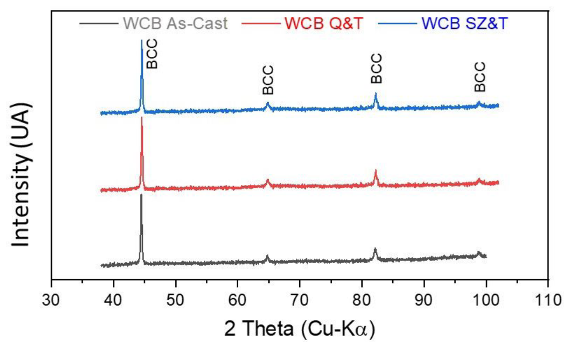


**Figure 16.** XRD of WCB as cast and after heat treatment.

it's possible to notice that in both samples without subzero quenching there is a decrease of the hardness in the interface, while in the WCB there is no perceptible change in hardness and a slight increase in the HCCI. The reduction in hardness in carbide particles can be mainly associated with the stress relieve subsequent of the heat treatments.

Figure 11 shows that for the sample subjected to subzero quenching once again that WCB hardness remains unchanged, while in the HCCI the hardness increases since less retained austenite is found after the subzero heat treatment. In Figure 12 and Figure 13 the hardness reduces a little but compared with the sample as received there are fewer points with hardness greater than 1800 HV, the distribution is more homogeneous reducing the general hardness of the sample. Tempering leads to a reduction in the hardness of the material, ensuring more toughness, while austenite guarantees greater resistance to wear, but reduces tool life[9,13-15]. In some studies[13], the tempering temperatures used were higher, varying between 350-420 °C and with times as long as 6 hours. With longer tempering times and higher temperatures, it may be possible to lower the hardness even more and gain toughness without losing too much abrasion resistance, since this property is given mainly by the carbide particles. Higher tempering temperatures ensure a more efficient hardening and better wear behavior, it also can form M2C carbides from the M7C3 particles[14,15].

Figure 14 shows the average values of the three areas from the component, as it can be seen, there is a decrease on the hardness in the interface after quenching and a increase in the HCCI. After tempering the hardness values of the HCCI decreases, which is the purpose of this heat treatment. The standard deviation of HCCI is higher because the elevate hardness of the M7C3carbides distributed at the matrix.

An important factor in carrying out heat treatments is to balance the microstructure in such a way that your component has the ideal properties for the chosen application[14-16]. In the case of the HCCI, a certain fraction of austenite is beneficial for the toughness of the material. Figure 15 presents the XRD results with the phase fractions calculated by means of Rietvled refinement. The as-cast and the subzero materials have very similar phase fractions. The quenched and tempered material (without subzero treatment) also shows a similar M7C3-type carbide volume fraction, but a considerably higher amount of retained austenite. Possibly with longer times and higher austenitization temperatures, it would be possible to increase even further the amount of austenite, as observed in other works[10,11,13]. In WCB, no difference is observed after heat treatments, as seen in Figure 16, which is good for a hybrid component, since both alloys will. Since these heat treatments did not affect negatively the properties of the WCB steel, this alloy is a good candidate to support material in hybrid castings using HCCI.

## 4. Conclusion

Hybrid casting is a new fabrication concept that can bring down the cost and production lead time of large tools, such as stamping tools for the automotive industry. In this work, we analyzed a hybrid material composed of a high chromium cast iron (HCCI) and a low carbon steel (WCB).

SEM analyses indicate that the interface is free of non-metallic inclusions and porosities. The metallurgical bonding between alloys is confirmed by the diffusion of chromium and carbon from HCCI to WCB. Vickers microhardness, EDS and XRD confirmed the presence of M7C3 carbides in the HCCI and at the interface. The material was submitted to two different sequences of quenching and tempering heat treatments, one of them involving a subzero quenching in liquid nitrogen.

In both cases, samples submitted to calm air quenching and subzero quenching, a slight reduction of the HCCI hardness and an increase of the interface hardness were observed. The subzero treatment was very effective to reduce the amount of retained austenite at the HCCI and limiting its hardness reduction. WCB microstructure and hardness showed no significative change, making it an ideal material to use together with HCCI in hybrid casts. The results showed that is possible to produce bimetallic reliable components for industrial applications by means of hybrid casting.

## 5. Acknowledgments

The author ELSJ acknowledges Fundação de Desenvolvimento de Pesquisa (FUNDEP) and the Rota 2030 Program for the scholarship and financial support to this study.

## 6. References

1. Wróbel T. Characterization of bimetallic castings with an austenitic working surface layer and an unalloyed cast steel base. J Mater Eng Perform. 2014;23(5):1711-7. http://dx.doi.org/10.1007/s11665-014-0953-4.
2. Ramadan M, Fathy N, Abdel Halim KS, Alghamdi AS. New trends and advances in bi-metal casting technologies. Int J Adv Appl Sci. 2019;6(2):75-80. http://dx.doi.org/10.21833/ijaas.2019.02.011.
3. Leibholz H, Leibholz R, Leibholz F, Leibholz A, Araújo M, Santos PO. Processo de fundição Hybrid® 1. Rev ABIFA. 2014;167:56.
4. Kopycinski D, Guzik E, Siekaniec D, Szczesny A. Analysis of the high chromium cast iron microstructure after the heat treatment. Arch Foundry Eng. 2014;14(3):43-6. http://dx.doi.org/ 10.2478/afe-2014-0059.
5. Wiengmoon A. Carbides in high chromium cast irons. Naresuan Univ Eng J. 2011;1:64-71.
6. Ibrahim KM, Ibrahim MM. Heat treatment in high chromium white cast iron Ti alloy. J Metall. 2014;2014:1-9. http://dx.doi.org/10.1155/2014/856408.
7. Jilleh A, Kishore Babu N, Thota V, Anis AL, Harun MK, Talari MK. Microstructural and wear investigation of high chromium white cast iron hardfacing alloys deposited on carbon steel. J Alloys Compd. 2021;857. http://dx.doi.org/10.1016/j.jallcom.2020.157472.
8. Li P, Yang Y, Shen D, Gong M, Tian C, Tong W. Mechanical behavior and microstructure of hypereutectic high chromium cast iron: the combined effects of tungsten, manganese and molybdenum additions. J Mater Res Technol. 2020;9(3):5735-48. http://dx.doi.org/10.1016/j.jmrt.2020.03.098.
9. Schaffnit P, Stallybrass C, Konrad J, Stein F, Weinberg M. A Scheil–Gulliver model dedicated to the solidification of steel. Calphad. 2015;48:184-8. http://dx.doi.org/10.1016/j.calphad.2015.01.002.
10. Hashimoto M, Kubo O, Matsubara Y. Analysis of carbides in multi-component white cast iron for hot rolling mill rolls. ISIJ Int. 2004;44(2):372-80. https://doi.org/10.2355/isijinternational.44.372.
11. Matsubara Y, Sasaguri N, Shimizu K, Yu K. Solidification and abrasion wear of white cast irons alloyed with 20% carbide forming elements. Wear. 2001;250(1-2):502-10. https://doi.org/10.1016/S0043-1648(01)00599-3.
12. Higuera-Cobos OF, Dumitru F-D, Mesa-Grajales DH. Improvement of abrasive wear resistance of the high chromium cast iron ASTM A-532 through thermal treatment cycles. Rev Fac Ing. 2016;25(41):93-103.
13. Doğan ÖN, Hawk JA, Laird G. Solidification structure and abrasion resistance of high chromium white irons. Metall Mater Trans, A Phys Metall Mater Sci. 1997;28(6):1315-28. http://dx.doi.org/10.1007/s11661-997-0267-3.
14. Belzunce Varela FJ, Fernández Pariente I. Influencia de diversos tratamientos térmicos en la microestructura de una fundicion blanca con alto contenido en cromo. Rev Metal. 2006;42(4):279-86.
15. Younes R, Sadeddine A, Bradai MA, Aissat S, Benabbas A. Investigation on the influence of tempering on microstructure and wear properties of high alloy chromium cast iron. Adv Mater Sci. 2021;21(2):65-76. http://dx.doi.org/10.2478/adms-2021-0011.
16. Prayogo RS, Setyana LD. The improvement of wear and impact resistance of high chromium white cast iron for crusher. J Mater Process Charact. 2020;1(2):96-102. http://dx.doi.org/10.22146/jmpc.68282.